

Characteristics of flake graphite in Ni-Mn-Cu cast iron. Part 2.

A. Janus

Department of Foundry and Automation, Institute of Mechanical Engineering and Automation,
Wrocław University of Technology,
ul. Wybrzeże Wyspiańskiego 27, 50-370 Wrocław, Polska

* Corresponding author. E-mail address: andrzej.janus@pwr.wroc.pl

Received 20.07.2009; accepted in revised form 27.07.2009

Abstract

The paper continues the article published by Archives of Foundry Engineering, vol. 9, issue 1/2009, pp. 185-290, that presented influence of chemical composition of hypo- and hypereutectic nickel-manganese-copper alloyed cast iron on properties of the contained flake graphite. In this second part of the research, effect of chemical composition of hypereutectic cast iron containing 3.5÷5.1% C, 1.7÷2.8% Si, 3.5÷10.5 %Ni, 2.0÷8.0% Mn, 0.1÷3.5% Cu, 0.14÷0.17% P and 0.02÷0.04% S on properties of flake graphite is determined. Evolution of graphite properties with changing eutecticity degree of the examined cast iron is presented. For selected castings, histograms of primary and eutectic graphite are presented, showing quantities of graphite precipitates in individual size ranges and their shape determined by the coefficient ξ defined as ratio of a precipitate area to square of its circumference. Moreover, presented are equations obtained by discriminant analysis to determine chemical composition of Ni-Mn-Cu cast iron which guarantee the most favourable distribution of A-type graphite from the point of view of castings properties.

Key words: Flake graphite; Austenitic cast iron; Ni-Mn-Cu cast iron

1. Introduction

Properties of castings made of hypo- and hypereutectic grey cast iron are significantly affected by size and branching degree of graphite skeletons formed during solidification of eutectic mixture [1÷3]. In hypereutectic cast iron, this effect is even stronger since graphite is a primary phase that can influence shape of eutectic colonies. This means that a change of features of solidifying graphite must cause a change of castings properties. It can be assumed that these features depend on overcooling degree of metal bath (in terms of temperature and concentration). One of the factors decisive for overcooling of solidifying cast iron is its chemical composition, first of all carbon concentration. However, role of the remaining elements can not be omitted, because they change carbon solubility in cast iron and can influence degree of local overcooling at the solidification front [4, 5].

Graphite can be described in various ways. With respect to complex shape of graphite precipitates, determined are features of cross-sections of graphite skeleton branches visible on the plane of a metallographic polished section. These cross-sections are treated as separate graphite precipitates. Shape, distribution and size of the precipitates are most frequently evaluated by comparison with reference standards included in technical specifications. In comparison to the previous PN-75/H-0466, the currently valid ISO EN-PN 945:1999 introduces significant classification restrictions. For this reason, this article partially uses the terminology and classification defined by PN-75/H-0466, commonly applied in literature.

For graphite evaluation, quantitative metallography methods using image analysers are also applied [6,7]. Despite numerous shortcomings, these methods are more and more often used, since they allow acquiring and analysing large data sets. Thanks to this,

it is possible to evaluate graphite by means of statistical methods which level distribution inhomogeneities in castings and permit considering variety of forms present in one graphite area. Computerised image analysis is most frequently used for determining graphite quantity and its shape index. In literature, this index is defined in various ways. It is most often defined as ratio of graphite precipitate area to square of its circumference. According to literature data, the ξ index ranges from 0 to 0.030 for flake graphite, from 0.035 to 0.065 for vermicular graphite and from 0.065 to 0.080 for modular graphite [7].

2. Purpose and scope of the research

The research was aimed at determining influence of chemical composition of austenitic Ni-Mn-Cu cast iron on properties of the occurring flake graphite. Examinations were performed on over a hundred castings with various chemical composition. For hypoeutectic and eutectic alloys, analysis was made in the first part of the work [8]. In the present part, effect of chemical composition of hypereutectic cast iron containing 3.5÷5.1% C, 1.7÷2.8% Si, 3.5÷10.5 %Ni, 2.0÷8.0% Mn, 0.1÷3.5% Cu, 0.14÷0.17% P and 0.02÷0.04% S on features of primary and eutectic graphite was analysed. Moreover, global effect of individual elements concentration on distribution of flake graphite was determined by statistical discriminant analysis.

Since graphite features are also decided by solidification rate, evaluated was graphite occurring in the areas ca. 10 mm away from surfaces of standard cylindrical castings dia. 30 mm. It was assumed that, because of this, changes of graphite features are merely related to chemical composition of cast iron.

3. Own research

In the examined hypereutectic alloys, the first clearly recognisable primary graphite precipitates occur in cast iron with the eutectic saturation coefficient S_c equal to ca. 1.10. At lower S_c values, number of these precipitates is small and their size is close to that of eutectic graphite. It is only in clearly hypereutectic alloys that the role of primary graphite precipitates becomes important. An example of cast iron with small quantity of primary graphite can be the alloy containing 4.06% C, 2.1% Si, 3.3% Ni, 5.8% Mn and 0.1% Cu, for that S_c is 1.09. It contains fine eutectic graphite and single precipitates of much larger, branched primary graphite, see Fig. 1a. Size of eutectic graphite precipitates is close to that of graphite present in extreme areas of eutectic colonies of hypoeutectic cast iron. Most of these precipitates are within 45 to 70 μm , see Fig. 1b. It is difficult to determine the size of primary graphite precipitates because of their branched shape. So, the method was accepted, according to that a precipitate size is equal to minimum diameter of the circle circumscribed on this precipitate. In most cases, a precipitate graphite size calculated by this method ranges from 150 to 250 μm , see Fig. 1c. Despite clear difference of sizes between eutectic and primary graphite precipitates, their shape index values differ slightly only. For eutectic graphite, the average ξ value is 0.017, but for primary graphite it is 0.015, see Fig. 19d. It results from this that increase

of primary graphite size is accompanied by immediate increase of flake thickness.

Further increasing the eutectic saturation coefficient S_c in hypereutectic cast iron leads to larger quantity and slightly larger size of primary graphite precipitations. Size and number of primary graphite precipitates do not change significantly. Fig. 2 shows structure and histograms of size and shape index of cast iron with the eutectic saturation coefficient equal to 1.40. This is an alloy containing 4.62% C, 2.0% Si, 6.6% Ni, 4.0% Mn and 2.8% Cu. With respect to size of precipitates (Fig. 2a, b), distinctly marked is division into eutectic graphite with precipitates 40 to 80 μm long and primary graphite whose most precipitates are not longer than 200 μm , see Fig. 2c. Number of the eutectic graphite precipitates exceeds that of primary graphite, but surface area occupied by the latter is much larger. The eutectic graphite (precipitates below 80 μm) covers ca. 10 % of total surface area occupied by graphite. For the primary graphite (precipitates over 200 μm) this is more than 65 %. Changes of graphite shape resulting from increase of the eutecticity degree are much smaller. Like in the case of cast iron with lower eutecticity degree, the shape index ξ of most graphite precipitates (ca. 70 %) ranges from 0.001 to 0.020, see Fig. 2d.

4. Summary

It results from the presented analysis of casting structures that within the assumed range of chemical composition some significant differences appear between features of precipitating graphite. Diversity of shapes, arrangements and sizes of graphite precipitates indicates a necessity of determining the range of chemical compositions to obtain graphite ensuring most favourable properties of cast iron. It seems that this will be guaranteed by the structure with dominating graphite type IA, as determined according to the standard. This means exclusion of the alloys containing mainly interdendritic graphite (arrangement type D) or with dominating excessively grown primary graphite precipitates.

The examined alloys were classified in three groups and subject to discriminant analysis. To the first group, the alloys partially chilled (completely chilled castings were not considered in the analysis) and those with prevailing graphite with interdendritic arrangement type D or E were counted. In the second group, the alloys with prevailing graphite arrangement type A were classified. The third group included the alloys with graphite arrangement type C (primary graphite precipitates covered more than 15 % of total graphite area on polished section surface). Finally, numbers of castings in individual groups were: group 1 – 39 alloys, group 2 – 32 alloys and group 3 – 21 alloys.

As a result of the discriminant analysis, the system of three equations was obtained:

$$\text{for the group No. 1:} \\ X_{\text{gr1}} = -87,07 + 26,50 \cdot C + 28,73 \cdot \text{Si} + 4,92 \cdot \text{Ni} - 1,60 \cdot \text{Mn} + 3,04 \cdot \text{Cu} \quad (1)$$

$$\text{for the group No. 2:} \\ X_{\text{gr2}} = -100,03 + 31,31 \cdot C + 28,20 \cdot \text{Si} + 5,22 \cdot \text{Ni} - 2,03 \cdot \text{Mn} + 2,84 \cdot \text{Cu} \quad (2)$$

for the group No. 3:

$$X_{gr1} = -133,36 + 38,08 \cdot C + 30,25 \cdot Si + 5,66 \cdot Ni - 2,26 \cdot Mn + 3,19 \cdot Cu \quad (3)$$

Wilks' lambda: 0.44; $p < 0.001$; approx. $F(5.87) = 24.1$
 $X_{gr1}, X_{gr2}, X_{gr3}$ – values of the equations
 C, Si, Ni, Mn, Cu – concentrations of individual elements

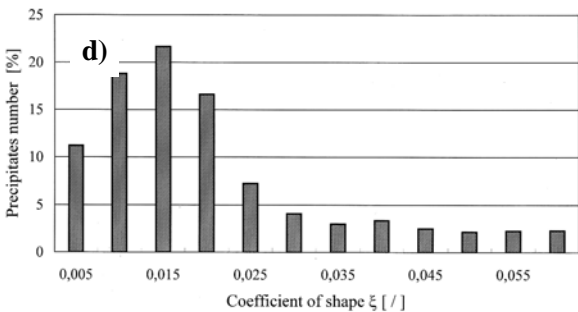
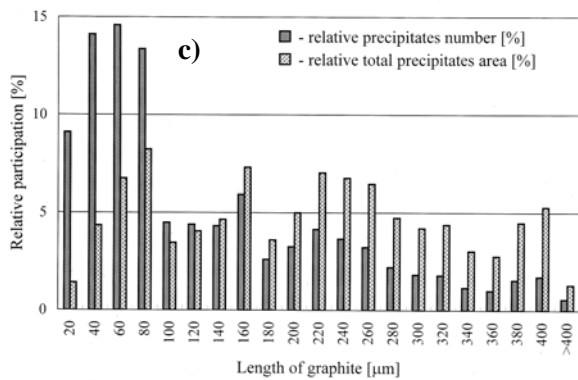
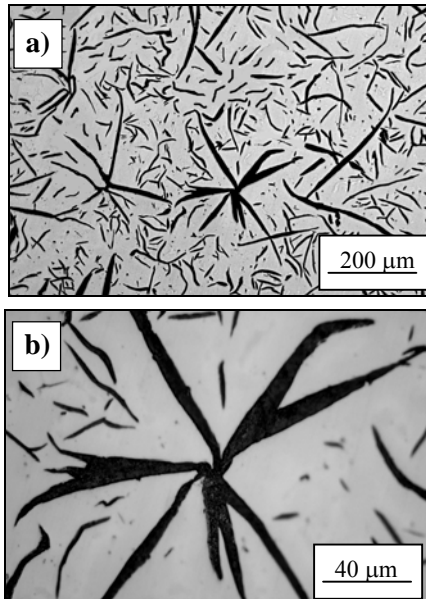


Fig. 1. Primary graphite and eutectic flake graphite in cast iron containing 4.06% C, 2.1% Si, 3.3% Ni, 5.8% Mn and 0.1% Cu, $S_c=1,09$: a), b) view of graphite, c) histogram of graphite precipitate sizes, d) histogram of graphite shape index ξ

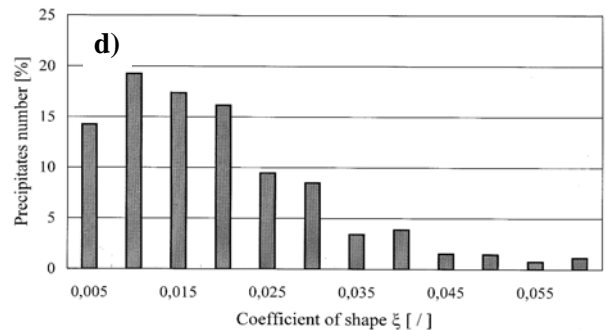
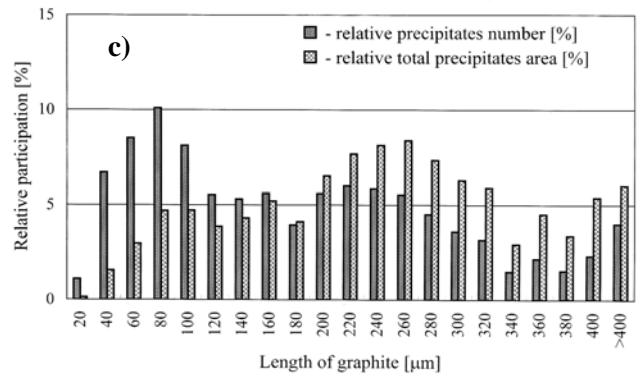
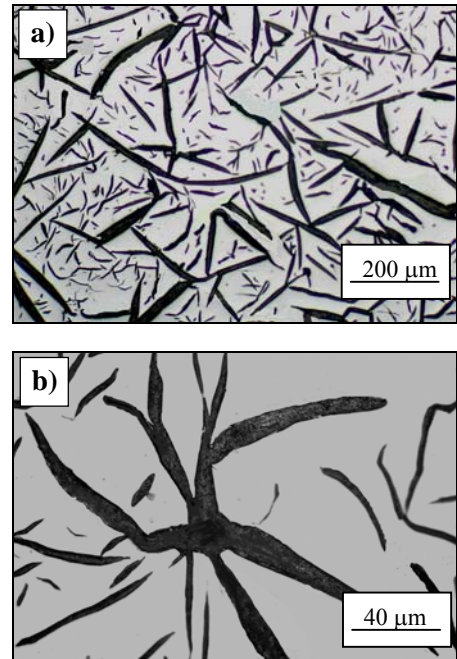


Fig. 2. Primary graphite and eutectic flake graphite in cast iron containing 4.62% C, 2.0% Si, 6.6% Ni, 4.0% Mn and 2.8% Cu, $S_c=1,40$: a), b) view of graphite, c) histogram of graphite precipitate sizes, d) histogram of graphite shape index ξ

Conformity of graphite shapes in the castings with the classification performed on the ground of the equations (1)÷(3) is illustrated by the classification matrix in Table 1. Incorrectly were classified eight alloys. This concerns 3 alloys of 39 in the first group, 4 alloys in the second group and 1 alloy in the third group.

Table 1.
Classification matrix of equations (1) ÷ (3)

	Correctly classification [%]	Number of casts		
		Group 1	Group 2	Group 3
Group 1	92	36	3	0
Group 2	88	3	28	1
Group 3	95	0	1	20
Summa		39	32	21

After rearranging the equations (1) ÷ (3) it is possible to determine the borders between the alloys of the individual groups. The system of equations accepts the form:

- border between the groups No. 1 and 2:

$$0,371 \cdot C - 0,041 \cdot Si + 0,023 \cdot Ni - 0,033 \cdot Mn - 0,015 \cdot Cu = 1$$

- border between the groups No. 2 and 3:

$$0,203 \cdot C + 0,061 \cdot Si + 0,013 \cdot Ni - 0,007 \cdot Mn + 0,010 \cdot Cu = 1$$

So, obtaining structures with prevailing graphite arrangement type A acc. to the standard requires such selection of individual elements concentrations that the value of the equation (4) is higher than 1 and the value of the equation (5) is lower than 1.

The absolute values of regression coefficients of the equations (4) and (5) indicate that the key role in shaping the graphite features is played by carbon. Higher value of the regression coefficient for this element in the equation (4) than in the equation (5) evidences that carbon influences the change of graphite arrangement from interdendritic type D or E to type A more intensively than from the arrangement type A to type C (with dominating primary graphite).

Influence of silicon on graphite features is several times weaker than influence of carbon. It results from evaluation of regression coefficients for this element in the equations (4) and (5) that its effect on obtaining the arrangement type A in the examined alloys should be recognised as unfavourable. By decreasing the value of (4) and increasing the value of (5) this element narrows the area of graphite arrangement type A.

Unlike silicon, nickel increases the values of both equations (4) and (5) which means that, at the same carbon concentration in cast iron, it simplifies the transition from interdendritic arrangement to the arrangement type A, but at the same time increases quantity of primary graphite.

Manganese acts in opposite direction. As a carbide-forming element it increases tendency of cast iron to crystallization of interdendritic graphite, at the same time decreasing quantity of

primary graphite in hypereutectic alloys. Intensity of this influence can be compared to that of nickel.

Copper, like silicon, is conducive to solidification of eutectic mixture with interdendritic graphite, at the same time slightly increasing quantity of primary graphite. Comparison of absolute values of the regression coefficients in both equations indicates that, among the examined elements, effect of copper on graphite features is the weakest.

References

- [1] J. V. Giacchi, R.A. Martínez, M.R. Gamba, R.C. Dommarco, Abrasion and impact properties of partially chilled gray iron, *Wear*, vol: 262, issue: 3-4, 2007, 282-291.
- [2] X.J. Sun, Y.X. Li, X. Chen, Identification and evaluation of modification level for compacted graphite cast iron, *Journal of Materials Processing Tech.*, vol: 200, issue: 1-3, 2008, 471-480.
- [3] E. Fraś, M. Górny, W. Kapturkiewicz, H. López, Chilling Tendency and Chill of Cast Iron, *Tsinghua Science & Technology*, vol: 13, issue: 2, 2008, 177-183.
- [4] B. Ceccarelli, R. Dommarco, R. Martinez, M. Gamba, M., Abrasion and impact properties of partially chilled ductile iron, *Wear* 2004 pp. 49-55.
- [5] R. Dommarco, M. Sousa, J. Sikora, Abrasion resistance of high nodule count ductile iron with different matrix microstructures, *Wear* 2004 pp. 1185-1192.
- [6] M. H. Cho, S.J. Kim, R. H. Basch, J. W. Fash, H. Jang, Tribological study of gray cast iron with automotive brake linings: The effect of rotor microstructure, *Unsubscribed Journal Tribology International*, vol: 36, issue: 7, 2003, 537-545.
- [7] Y. Zhang, Y. Chen, R. He, B. Shen, Investigation of tribological properties of brake shoe materials-phosphorous cast irons with different graphite morphologies, *Wear* 1993, pp. 179-186.
- [8] A.R. Ghaderi, M. Ahmadabadi, H.M. Ghasemi, Effect of graphite morphologies on the tribological behavior of cast iron, *Wear*, vol: 255, issue: 1-6, 2003, 410-416.
- [9] Y. Wang, X. Wei, Jing, M. Tianfu, S. J. Gao, Y. Xin, "Properties of a gray cast iron with oriented graphite flakes" *Journal of Materials Processing Tech.* 2007, 593-597.
- [10] C. Podrzucki, *Cast Iron. Structure, properties, application*, ZG STOP, Kraków, 1991.
- [11] E. Fraś, *Crystallization of metals*, WNT, W-wa 2003.
- [12] T. Warchala, M. S. Soiński, Charakterystyka wydzieleniu grafitu w żeliwie modyfikowanym dodatkami bizmutu i metali ziem rzadkich, *Archives of Mechanical Technology and Automatization*, vol. 18, inssue: specjal, 1998, 297-306.
- [13] A. Janus, K. Granat, Austenityczno-bainityczne żeliwo Ni-Mn-Cu odporne na ścieranie, *Raporty Inst. Technol. Masz. Autom. PWroc.* 2005 Ser. SPR nr 28.